Eur. Phys. J. A **21**, 445–454 (2004)
DOI 10.1140/epja/i2004-10003-3

THE EUROPEAN PHYSICAL JOURNAL A

Spin-$\frac{5}{2}$ resonance contributions to the pion-induced reactions for energies $\sqrt{s} \leqslant 2.0\,\mathrm{GeV}^{\star}$

V. Shklyar[a], G. Penner, and U. Mosel

Institut für Theoretische Physik, Universität Giessen, D-35392 Giessen, Germany

Received: 30 January 2004 / Revised version: 26 February 2004 /
Published online: 31 August 2004 –
Communicated by V. Vento

Abstract. The spin-$\frac{5}{2}$ resonance effects are studied within the coupled-channel effective Lagrangian model for baryon resonance analysis. We extend our previous hadronic calculations to incorporate the D_{15}, F_{15}, D_{35}, F_{35} states. While the effect of the spin-$\frac{5}{2}$ resonances to the ηN, $K\Lambda$, and $K\Sigma$ reactions is small, the contribution to the ωN is found to be important. The results for the "conventional" and Pascalutsa-like spin-$\frac{5}{2}$ descriptions are discussed.

PACS. 11.80.-m Relativistic scattering theory – 13.75.Gx Pion-baryon interactions – 14.20.Gk Baryon resonances with $S = 0$

1 Introduction

The extraction of baryon resonance properties is one of the important tasks of modern hadron physics. Great efforts have been made in the past to obtain this information from the analysis of pion- and photon-induced–reaction data. The precise knowledge of these properties is an important step towards understanding the hadron structure and finally the strong interactions.

Some quark models (see [1] and references therein) predict that the baryon resonance spectrum may be richer than discovered so far. This is the so-called problem of "missing" nucleon resonances. One assumes that these states are weakly coupled to pion channels and are consequently not clearly seen in πN, $2\pi N$ and ηN reactions from which experimental data are most often used for baryon resonance analyses. To incorporate other possible finale states a unitary coupled-channel model (Giessen model) has been developed which includes γN, πN, $2\pi N$, ηN, $K\Lambda$ final states and deals with all available experimental data on pion- and photon-induced reactions [2,3]. The most recent extensions of this model include $K\Sigma$ and ωN final states [4–6] as well, which allows for the simultaneous analysis of all hadronic and photoproduction data up to $\sqrt{s} = 2\,\mathrm{GeV}$. A shortcoming of this study is the missing of higher-spin resonances with spin $J > \frac{3}{2}$. Since the spin-$\frac{5}{2}$ resonances have large electromagnetic couplings [7–9], this limited the previous analysis of the Compton scattering data to the energy region $\sqrt{s} \leqslant 1.6\,\mathrm{GeV}$. Moreover, the extension to higher-spin baryon spectra becomes unavoidable for investigation of "hidden" or "missing" nucleon resonances. In particular, a study of the spin-$\frac{5}{2}$ part of the baryon spectra can shed light on the dynamics of the vector (ω and ρ) meson production mechanisms which is itself a very intriguing question (see [10] and references therein).

In the present paper we study the effect of spin-$\frac{5}{2}$ resonance contributions to πN, $2\pi N$, ηN, $K\Lambda$, $K\Sigma$, and ωN final states. Starting from the effective Lagrangian coupled-channel model [5] we extend our previous hadronic calculation [5] by including the D_{15}, F_{15}, D_{35}, F_{35} resonances and simultaneously analysing all available pion-induced–reaction data in up to the 2 GeV energy region. Due to the coupled-channel calculations this model provides a stringent test for the resonance contributions to the all open final states. Similar to the spin-$\frac{3}{2}$ case in [5,6], the contributions from spin-$\frac{5}{2}$ states are investigated for two different types of the spin-$\frac{5}{2}$ couplings: for the "conventional" (C) and Pascalutsa (P) prescriptions. While the first approach dates back to the original work of Rarita and Schwinger [11] and is widely used in the literature, the latter one assumes the gauge-invariant resonance coupling. Although the data quality is not good enough to distinguish between these two pictures now, this question is challenging for an understanding of the meson-baryon interactions. With this aim in mind, the present work extends our earlier multi-channel analysis based on an effective Lagrangian approach by including also the spin-$\frac{5}{2}$ resonances.

⋆ Supported by DFG and GSI Darmstadt.
[a] e-mail: shklyar@theo.physik.uni-giessen.de

The paper is organized as follows. We start in sect. 2 with a description of the formalism concentrating mainly on the spin-$\frac{5}{2}$ couplings; the complete discussion of our model including all other couplings can be found in [5,6,12]. In sect. 3 we discuss the results of our calculations in comparison with the previous studies [5] and finish with a summary (sect. 4).

2 The Giessen model

We solve the Bethe-Salpeter coupled-channel equation in the K-matrix approximation to extract scattering amplitudes for the final states under consideration. The validity of the K-matrix approximation has been tested by Pearce and Jennings who have performed a fit to the elastic πN phase shifts up to 1.38 GeV with the "smooth", Blankenbecler-Sugar and the K-matrix propagators [13]. They have found no significant differences in the parameters extracted in the three cases. Also, a successful description of the pion- and photon-induced–reaction data [5,6] and η production [14] points to the applicability of this approximation for investigation of the baryon resonance spectra.

In order to decouple the equations we perform a partial-wave decomposition of the T-matrix into total spin J, isospin I, and parity $P = (-1)^{J\pm\frac{1}{2}}$. Then the partial-wave amplitudes can be expressed in terms of an interaction potential $\mathcal{K}$ via the matrix equation

$$\mathcal{T}^{I,J\pm} = \left[\frac{\mathcal{K}^{I,J\pm}}{1 - \mathrm{i}\mathcal{K}^{I,J\pm}}\right], \tag{1}$$

where each element of the matrices $\mathcal{T}_{fi}^{I,J\pm}$ and $\mathcal{K}_{fi}^{I,J\pm}$ corresponds to a given initial and final state ($i, f = \pi N$, $2\pi N$, ηN, $K\Lambda$, $K\Sigma$, ωN). The interaction potential is approximated by tree-level Feynman diagrams which in turn are obtained from effective Lagrangians [5,12]. The $\mathcal{T}$-matrix (1) fulfils unitarity as long as the $\mathcal{K}$-matrix is Hermitian. In our model the following 19 resonances are included: $P_{33}(1232)$, $P_{11}(1440)$, $D_{13}(1520)$, $S_{11}(1535)$, $P_{33}(1600)$, $S_{31}(1620)$, $S_{11}(1650)$, $D_{15}(1675)$, $F_{15}(1680)$, $D_{33}(1700)$, $P_{11}(1710)$, $P_{13}(1720)$, $P_{31}(1750)$, $P_{13}(1900)$, $P_{33}(1920)$, $F_{35}(1905)$, $D_{35}(1930)$, $F_{15}(2000)$, and $D_{13}(1950)$, which is denoted as $D_{13}(2080)$ by the PDG [7].

The Lagrangian for the spin-$\frac{5}{2}$ resonance decay to a final baryon B and a (pseudo)scalar meson φ is chosen in the form

$$\mathcal{L}^{\frac{5}{2}}_{\varphi BR} = \frac{\mathrm{g}_{\varphi BR}}{m_\pi^2}\bar{u}_R^{\mu\nu}\Theta_{\mu\delta}(a)\Theta_{\nu\lambda}(a')\Gamma_S u_B \partial^\delta\partial^\lambda\varphi + \mathrm{h.c.} \tag{2}$$

with the matrix $\Gamma_S = \mathbb{1}$ if resonance and final meson have identical parity and $\Gamma_S = \mathrm{i}\gamma_5$ otherwise. The off-shell projector $\Theta_{\mu\nu}(a)$ is defined by

$$\Theta_{\mu\nu}(a) = \mathrm{g}_{\mu\nu} - a\gamma_\mu\gamma_\nu, \tag{3}$$

where a is a free off-shell parameter. Since the on-shell symmetric spin-$\frac{5}{2}$ field $u_R^{\mu\nu}$ has to obey the Dirac equation and satisfies the conditions $\gamma_\mu u_R^{\mu\nu} = \partial_\mu u_R^{\mu\nu} = \mathrm{g}_{\mu\nu}u_R^{\mu\nu} = 0$ [11] the second part in (3) only contributes for off-shell particles, giving rise to lower-spin off-shell components in (2). In general the interaction Lagrangian (2) can have two off-shell projectors matched with both vector indices of the resonance field tensor. However, as we will see later, a good description of the experimental data can be achieved already with a single parameter a keeping the second one equal to zero. Thus, to keep our model as simple as possible we use only one off-shell projector in (2).

The widths of the hadronic resonance decays as extracted from the Lagrangian (2) are

$$\Gamma_\pm(R_{\frac{5}{2}} \to \varphi B) = I\frac{\mathrm{g}^2_{\varphi BR}}{30\pi m_\pi^4}k_\varphi^5\frac{E_B \mp m_B}{\sqrt{s}}\,. \tag{4}$$

The upper sign corresponds to the decay of a resonance into a meson with the identical parity and vice versa. I is the isospin factor and k_φ, E_B, and m_B are the meson momentum, energy and mass of the final baryon, respectively.

The coupling of the spin-$\frac{5}{2}$ resonances to the ωN final state is chosen to be

$$\begin{aligned}\mathcal{L}^{\frac{5}{2}}_{\omega N} = \bar{u}_R^{\mu\lambda}\Gamma_V\left(\frac{\mathrm{g}_1}{4m_N^2}\gamma^\xi + \mathrm{i}\frac{\mathrm{g}_2}{8m_N^3}\partial_N^\xi + \mathrm{i}\frac{\mathrm{g}_3}{8m_N^3}\partial_\omega^\xi\right)\\ \times\left(\partial_\xi^\omega \mathrm{g}_{\mu\nu} - \partial_\mu^\omega \mathrm{g}_{\xi\nu}\right)u_N\partial_\lambda^\omega\omega^\nu + \mathrm{h.c.},\end{aligned} \tag{5}$$

where the matrix Γ_V is $\mathbb{1}$ ($\mathrm{i}\gamma_5$) for positive (negative) resonance parity and ∂_N^μ (∂_μ^ω) denotes the partial derivative of the nucleon and the ω-meson fields, respectively. The above Lagrangian is constructed in the same manner as the one for spin-$\frac{3}{2}$ in [5]. Similar couplings were also used to describe electromagnetic processes [10,15–17]. Since the different parts of (5) contribute at different kinematical conditions we keep all three couplings as free parameters and vary them during the fit. The helicity amplitudes for the decay $R \to \omega N$ are given by

$$\begin{aligned}A^{\omega N}_{\frac{3}{2}} &= \frac{\sqrt{E_N \pm m_N}}{\sqrt{5m_N}}\frac{k_\omega}{4m_N^2}\Big(-\mathrm{g}_1(m_N \mp m_R)\\ &\quad + \mathrm{g}_2\frac{(m_R E_N - m_N^2)}{2m_N} + \mathrm{g}_3\frac{m_\omega^2}{2m_N^2}\Big),\\ A^{\omega N}_{\frac{1}{2}} &= \frac{\sqrt{E_N \pm m_N}}{\sqrt{10m_N}}\frac{k_\omega}{4m_N^2}\Big(\mathrm{g}_1(m_N \pm (m_R - 2E_N))\\ &\quad + \mathrm{g}_2\frac{(m_R E_N - m_N^2)}{2m_N} + \mathrm{g}_3\frac{m_\omega^2}{2m_N^2}\Big),\\ A^{\omega N}_{0} &= \frac{\sqrt{(E_N \pm m_N)}}{\sqrt{5m_N}}\frac{k_\omega m_\omega}{4m_N^2}\Big(\mathrm{g}_1 \pm \mathrm{g}_2\frac{E_N}{2m_N}\\ &\quad \pm \mathrm{g}_3\frac{(m_R - E_N)}{2m_N}\Big),\end{aligned} \tag{6}$$

with the upper (lower) signs corresponding to positive (negative) resonance parity. The lower indices stand for the helicity λ of the final ωN state $\lambda = \lambda_V - \lambda_N$, where we use an abbreviation as follows: $\lambda = 0 : 0 + \frac{1}{2}$, $\frac{1}{2} : 1 - \frac{1}{2}$, $\frac{3}{2} : 1 + \frac{1}{2}$. The resonance ωN decay width $\Gamma^{\omega N}$ can be

written as the sum over the three helicity amplitudes given above:

$$\Gamma^{\omega N} = \frac{2}{(2J+1)} \frac{k_\omega m_N}{2\pi m_R} \sum_{\lambda=0}^{3/2} \left| A_\lambda^{\omega N} \right|^2, \tag{7}$$

where $J = \frac{5}{2}$ for the spin-$\frac{5}{2}$ resonance decay.

For practical calculations we adopt the spin-$\frac{5}{2}$ projector in the form

$$\begin{aligned} P^{\mu\nu,\rho\sigma}_{\frac{5}{2}}(q) = {} & \frac{1}{2}(T^{\mu\rho}T^{\nu\sigma} + T^{\mu\sigma}T^{\nu\rho}) - \frac{1}{5}T^{\mu\nu}T^{\rho\sigma} \\ & + \frac{1}{10}\big(T^{\mu\lambda}\gamma_\lambda\gamma_\delta T^{\delta\rho}T^{\nu\sigma} + T^{\nu\lambda}\gamma_\lambda\gamma_\delta T^{\delta\sigma}T^{\mu\rho} \\ & + T^{\mu\lambda}\gamma_\lambda\gamma_\delta T^{\delta\sigma}T^{\nu\rho} + T^{\nu\lambda}\gamma_\lambda\gamma_\delta T^{\delta\rho}T^{\mu\sigma}\big), \end{aligned} \tag{8}$$

with

$$T^{\mu\nu} = -\mathrm{g}^{\mu\nu} + \frac{q^\mu q^\nu}{m_R^2}, \tag{9}$$

which has also been used in an analysis of the $K\Lambda$ photoproduction [16].

As is well known the description of particles with spin $J > \frac{1}{2}$ leads to a number of different propagators which have non-zero off-shell lower-spin components. To control these components the off-shell projectors (3) are usually introduced. There were attempts to fix the off-shell parameters and remove the spin-$\frac{1}{2}$ contribution in the case of spin-$\frac{3}{2}$ particles [18]. However, it has been shown [19] that these contributions cannot be suppressed for any value of a. Indeed, Read [20] has demonstrated that the choice of the off-shell parameter in the coupling is closely linked to the off-shell behavior of the propagator. To overcome this problem Pascalutsa suggested gauge invariance as an additional constraint to fix the interaction Lagrangians for higher spins and remove the lower-spin components [21]. Constructing the spin-$\frac{3}{2}$ interaction for a Rarita-Schwinger field $u^\mu_{\frac{3}{2}}$ by only allowing couplings to the gauge-invariant field tensor $U^{\mu\nu}_{\frac{3}{2}} = \partial^\mu u^\nu_{\frac{3}{2}} - \partial^\nu u^\mu_{\frac{3}{2}}$ Pascalutsa derived an interaction which (for example) for the $\pi N\Delta$ coupling is

$$\mathcal{L}_{\pi N\Delta} = f_\pi \bar{u}_N \gamma_5 \gamma_\mu \widetilde{U}^{\mu\nu} \partial_\nu \varphi + \text{h.c.}, \tag{10}$$

where $\widetilde{U}^{\mu\nu}$ is the tensor dual to $U^{\mu\nu}$: $\widetilde{U}^{\mu\nu} = \varepsilon^{\mu\nu\lambda\rho} U_{\lambda\rho}$ and $\varepsilon^{\mu\nu\lambda\rho}$ is the Levi-Civita tensor. The same arguments can also be applied to spin-$\frac{5}{2}$ particles. In this case the amplitude of meson-baryon scattering can be obtained from the conventional amplitude by the replacement

$$\begin{aligned} & \Gamma_{\mu\nu}(p',k') \frac{P^{\mu\nu,\rho\sigma}_{\frac{5}{2}}(q)}{\not{q} - m_R} \Gamma_{\rho\sigma}(p,k) \\ & \longrightarrow \Gamma_{\mu\nu}(p',k') \frac{\mathcal{P}^{\mu\nu,\rho\sigma}_{\frac{5}{2}}(q)}{\not{q} - m_R} \Gamma_{\rho\sigma}(p,k) \frac{q^4}{m_R^4}, \end{aligned} \tag{11}$$

where $\Gamma_{\rho\sigma}(p,k)$ are vertex functions that follow from (2) and (5) by applying Feynman rules and the projector $\mathcal{P}^{\mu\nu,\rho\sigma}_{\frac{5}{2}}(q)$ is obtained from (8), (9) by the replacement

$$q^\mu q^\nu / m_R^2 \longrightarrow q^\mu q^\nu / q^2.$$

This procedure is similar to that which has been used in the spin-$\frac{3}{2}$ case [21]. It has been shown for the spin-$\frac{3}{2}$ case [22], that both prescriptions are equivalent in the effective Lagrangian approach as long as additional contact interactions are taken into account when the Pascalutsa couplings are used. The differences between these descriptions have been discussed in [5,23,24] and here we perform calculations by using both "conventional" (C) and Pascaluta (P) approaches. Similar to the spin-$\frac{3}{2}$ case [20], the off-shell parameters a in (3) can be linked to the coupling strengths extracted through (6)

In order to take into account the internal structure of mesons and baryons each vertex is dressed by a corresponding form factor:

$$F_p\left(q^2, m^2\right) = \frac{\Lambda^4}{\Lambda^4 + (q^2 - m^2)^2}. \tag{12}$$

Here q is the four-momentum of the intermediate particle and Λ is a cutoff parameter. In [5] it has been shown that the form factor (12) gives systematically better results as compared to other ones, therefore we do not use any other forms for $F(q^2)$. The cutoffs Λ in (12) are treated as free parameters and allowed to be varied during the calculation. However, we demand the same cutoffs in all channels for a given resonance spin J: $\Lambda^J_{\pi N} = \Lambda^J_{\pi\pi N} = \Lambda^J_{\eta N} = \ldots$ etc., ($J = \frac{1}{2},\ \frac{3}{2},\ \frac{5}{2}$). This greatly reduces the number of free parameters; *i.e.* for all spin-$\frac{5}{2}$ resonances there is only one cutoff $\Lambda_{\frac{5}{2}}$ for all decay channels.

To take into account contributions of the $2\pi N$ channel in our calculations we use the inelastic partial-wave cross-section $\sigma^{JI}_{2\pi N}$ data extracted in [25]. To this end the inelastic $2\pi N$ channel is parameterized by an effective ζN channel where ζ is an effective isovector meson with mass $m_\zeta = 2m_\pi$. Thus ζN is considered as a sum of different ($\pi\Delta$, ρN, etc.) contributions to the total $2\pi N$ flux. We allow only resonance ζN couplings since each background diagram would introduce a meaningless coupling parameter. Despite this approximation the studies [2,3,14,5] have achieved a good description of the total partial-wave cross-sections [25] and we proceed in our calculations by using the above prescription. For the $R \to \zeta N$ interaction the same Lagrangians are used as for the $R \to \pi N$ couplings taking into account the positive parity of the ζ-meson.

3 Results and discussion

We use the same database as in [5] with additional elastic πN data for the spin-$\frac{5}{2}$ partial-wave amplitudes taken from the VPI group analysis [26]. For the $2\pi N$ channel we use the spin-$\frac{5}{2}$ partial-wave cross-sections derived in [25]. We confine ourselves to the energy region $m_\pi + m_N \leqslant \sqrt{s} \leqslant 2\,\text{GeV}$. The database on the ηN, $K\Lambda$, $K\Sigma$ and ωN channels incorporates all available experimental information from the pion threshold up to the 2 GeV energy region. This includes partial and differential cross-sections and polarisation measurements. The references on these reactions, 34 in total, are summarized in [12].

Table 1. χ^2 of the C (first line) and P fits (second line). The D_{35} πN and $2\pi N$ data have not been taken into account (see text).

Fit	Total π	$\chi^2_{\pi\pi}$	$\chi^2_{\pi 2\pi}$	$\chi^2_{\pi\eta}$	$\chi^2_{\pi\Lambda}$	$\chi^2_{\pi\Sigma}$	$\chi^2_{\pi\omega}$
C	2.60	2.60	7.63	1.37	2.14	1.83	1.23
P	3.65	3.80	10.06	1.75	2.54	2.93	1.83

The results presented in the following are from ongoing calculations to describe the data in all channels simultaneously. The resulting χ^2 of our best overall hadronic fits are given in table 1. The obtained $\chi^2_{\pi\pi}$ and $\chi^2_{\pi 2\pi}$ are calculated using experimental data from all πN and $2\pi N$ partial waves up to spin-$\frac{5}{2}$ except the D_{35}-wave. We find a problem with the description of the D_{35} partial wave so the resulting $\chi^2_{\pi\pi}$ turns out to be very large. Hence the $\chi^2_{\pi\pi}$ values given in table 1 are calculated by neglecting the πN data points for the D_{35} partial wave. From table 1 one can conclude that the C-prescription leads to a better description of the data in all partial waves. Note, that since the P-coupling does not have "off-shell" background we also include additional $D_{13}(1700)$ and $S_{31}(1900)$ resonances in the P-calculations [5,6].

Compared to the previous best hadronic fits C-p-$\pi+$ and P-p-$\pi+$ from [5,6], we obtain the same values for cutoffs and non-resonant couplings. The only exception is the $\Lambda_{\frac{1}{2}} = 2.79$ for the C-coupling which is less than that of C-p-$\pi+$. In addition we find $g_{NN\omega} = 4.59(4.20)$ and $\kappa_{NN\omega} = -0.12(0.06)$ for $C(P)$-coupling calculations which slightly differ from [5]. The results for the πN partial-wave amplitudes are shown in figs. 1, 2 in comparison with C-p-$\pi+$ result from [5]. We do not show here the corresponding P-p-$\pi+$ result since it almost coincides with the new P-calculations. The main differences are found for the conventional coupling calculations in comparison with the previous study. A substantially better description in the P_{13} partial wave is due to the additional off-shell background generated by spin-$\frac{5}{2}$ resonances. The same effect also improves the description of the real and imaginary high-energy tails of the P_{31} and S_{31} amplitudes, respectively. The contribution from the spin-$\frac{5}{2}$ resonances can also be seen in the D_{33} amplitude which is also affected by spin-$\frac{5}{2}$ off-shell components. This leads to a worsening in the imaginary part of D_{33} above 1.8 GeV, giving however improvement in the corresponding real part.

The $D_{15}(1675)$, $F_{15}(1680)$, and $F_{35}(1905)$ resonances were included in our calculations. We have also found evidence for a second F_{15} state around 1.98 GeV which is rated two-star by [7]. The results for $\pi N \to 2\pi N$ partial-wave cross-sections are shown in fig. 3. We stress that the πN partial-wave inelasticities are not fitted but obtained as a sum of the individual contributions from all open channels.

In the following each spin-$\frac{5}{2}$ wave is discussed separately. The extensive discussion of the spin-$\frac{1}{2}$ and spin-$\frac{3}{2}$ partial waves can be found in [5,6]. The parameters of the corresponding baryon resonances are listed in [27].

$\mathsf{D_{15}}$. The elastic VPI data show a single resonant peak which corresponds to the well-established $D_{15}(1675)$ state. We find a good description of the elastic amplitude in both the C- and P-calculations.

The $2\pi N$ data [25] are systematically below the total inelasticity of the VPI group [26]. This can be an indication that apart from $2\pi N$ there are additional contributions from other inelastic channels. However, in the analysis of Manley and Saleski [28] as well as in the most recent study of Vrana *et al.* [29] the total inelasticity in the D_{15}-wave is entirely explained by the resonance decay to the $\pi\Delta$ channel. We also find no significant contributions from the ηN, $K\Lambda$, $K\Sigma$, and ωN channels to the total πN inelasticity in the present hadronic calculations. The calculated $2\pi N$ cross-sections are found to be substantially above the data from [25] in all fits. Indeed, the difference between the $2\pi N$ and inelasticity data runs into 2 mb at 1.67 GeV. This flux can be absorbed neither by ηN, $K\Lambda$, $K\Sigma$, ωN channels, see fig. 4. Thus we conclude that either the πN and $2\pi N$ data are inconsistent with each other or other open channels (as $3\pi N$) must be taken into account. To overcome this problem and to describe the πN and $2\pi N$ data in the D_{15} partial wave the original $2\pi N$ data error bars [25] were enlarged by a factor 3. The same procedure was also used by Vrana *et al.* [29] and Cutkosky *et al.* [30] to fit the inelastic data.

In both C- and P-coupling calculations the total inelasticities in the D_{15}-wave almost coincide with the partial-wave cross-sections and therefore are not shown in fig. 3 (left top). A good description of the inelasticity in the D_{15}-wave is achieved and the extracted resonance parameters are also in agreement with other findings (see next section).

$\mathsf{F_{15}}$. The $F_{15}(1680)$ and $F_{15}(2000)$ resonances are identified in this partial wave. The inclusion of the second resonance significantly improves the description of the πN and $2\pi N$ experimental data in the higher-energy region. Some evidence for this state was also found in earlier works [28,31]. A visible inconsistency between the inelastic VPI data and the $2\pi N$ cross-section from [25] above 1.7 GeV can be seen in fig. 3 (left bottom). The three data points at 1.7, 1.725, and 1.755 GeV have, therefore, not been included in our calculations. Finally we achieve a reasonable description for both πN and $2\pi N$ data. The C- and P-coupling calculations give approximately the same results.

$\mathsf{F_{35}}$. A single resonance state $F_{35}(1905)$ was taken into account. Some other models find an additional lower-lying resonance with a mass of about 1.75 GeV [28,32,31,29]. However, we already find a good description of the elastic πN amplitudes and the $2\pi N$ cross-sections by only including the single $F_{35}(1905)$ state. The inclusion of a second state with somewhat lower mass leads to a worse description of the πN and $2\pi N$ data due to the strong interference between the two nearby states. The two $2\pi N$ data points at 1.87 and 1.91 GeV, which are apparently above the total inelasticity, have not been included in the calculations.

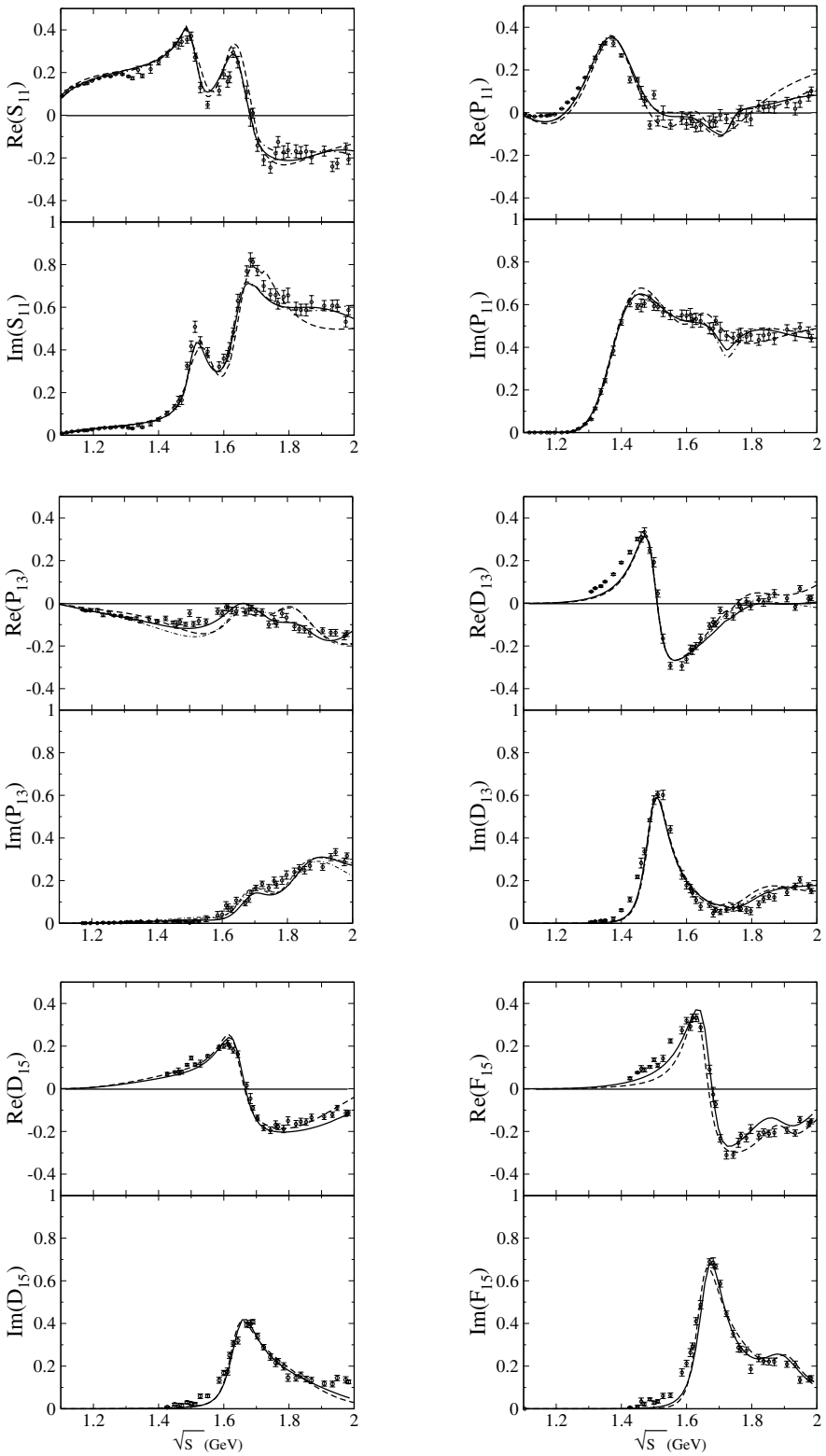

Fig. 1. The $\pi N \to \pi N$ partial waves for $I = \frac{1}{2}$. The solid (dashed) line corresponds $C(P)$-calculations. The dash-dotted line is the best hadronic fit C-p-$\pi+$ from [5]. The data are taken from [26].

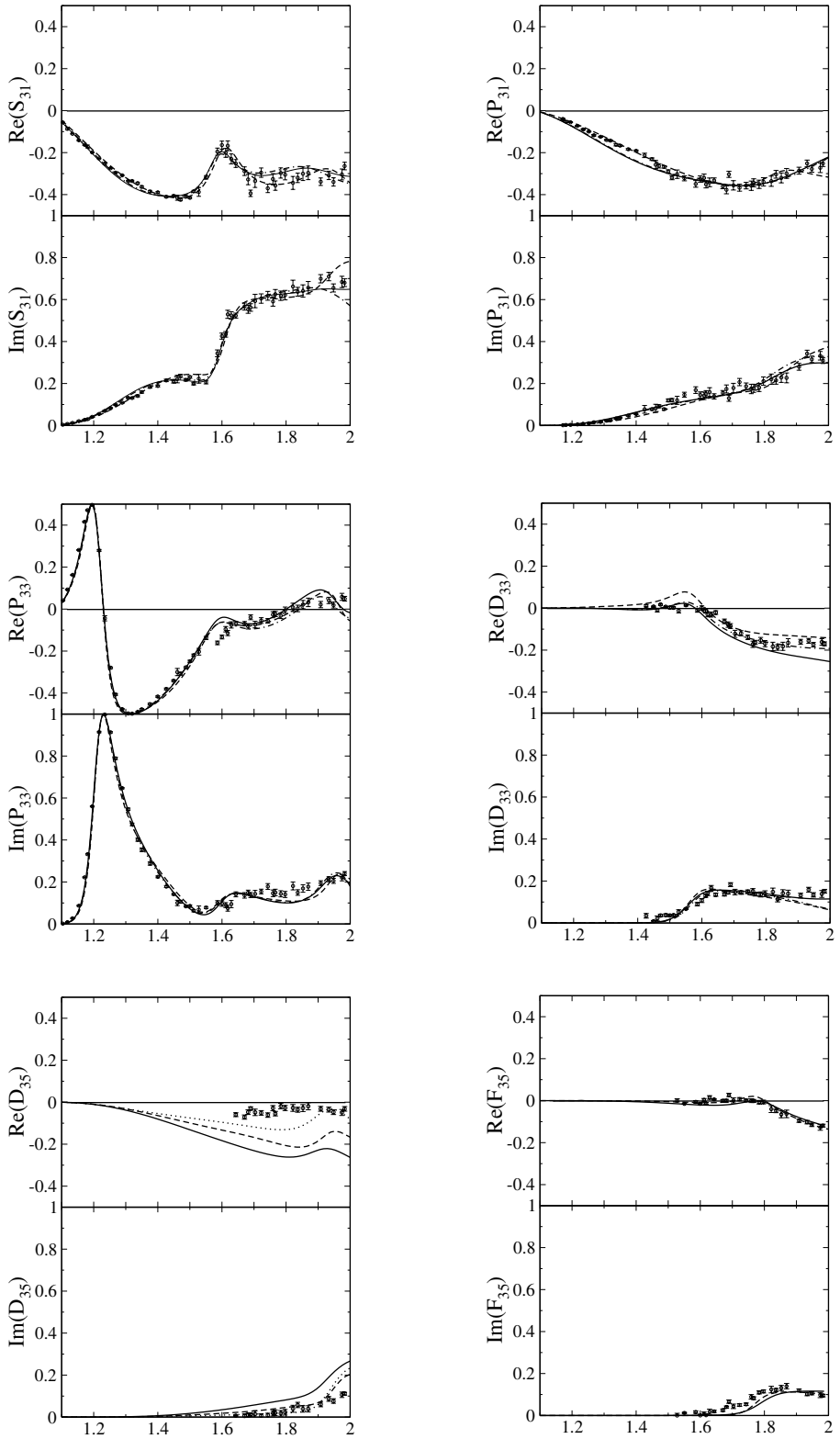

Fig. 2. The $\pi N \to \pi N$ partial waves for $I = \frac{3}{2}$. The solid (dashed) line corresponds $C(P)$-calculations. The dash-dotted line is the best hadronic fit C-p-π+ from [5]. The dotted line is the result for the D_{35}-wave obtained with reduced nucleon cutoff (see text). The data are taken from [26].

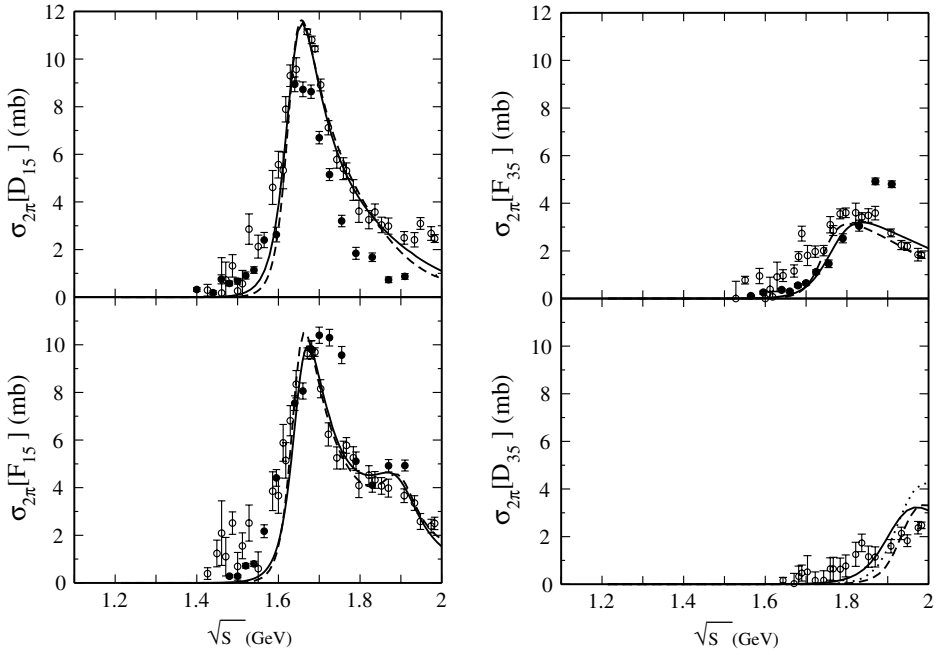

Fig. 3. The inelastic D_{15}, F_{15}, F_{35}, and D_{35} waves. The solid (dashed) line corresponds to calculation C (P) for the $2\pi N$ channel. Open and filled circles represent the total inelasticity from the VPI group [26] and the $2\pi N$ data [25], respectively. The calculated inelasticities almost coincide with the calculated $2\pi N$ cross-sections and are not shown here. Calculation with a reduced nucleon cutoff is shown by the dotted line.

The total inelasticity in the F_{35} partial wave almost coincides with the calculated $2\pi N$ cross-section and is not shown in fig. 3. Note, that the $2\pi N$ data at 1.7 GeV are slightly below the total inelasticity from [26]. This could indicate that other inelastic channels (as $3\pi N$) give additional contributions to this partial wave.

There are also difficulties in the description of the $2\pi N$ low-energy tails of the D_{15} and F_{15} partial waves below 1.6 GeV, where the calculated cross-sections are slightly below the $2\pi N$ data. The discrepancy leads to a significant rise in $\chi^2_{\pi 2\pi}$ (cf. table 1). The same behavior has been found in our previous calculations for the D_{I3} partial waves [5]. There, it has been suggested that the problem might be caused by the description of the $2\pi N$ channel in terms of an effective ζN state. Indeed, the findings of [28,29] show strong $\pi\Delta$ decay ratios in all three D_{15}, F_{15}, and F_{35} partial waves. The description of the $2\pi N$ channel in terms of the ρN and $\pi\Delta$ channels may change the situation when taking into account the ρN and $\pi\Delta$ phase spaces and corresponding spectral functions. Upcoming calculations will address this question.

$\mathsf{D_{35}}$. A single $D_{35}(1930)$-resonance is taken into account. However, there is no clear resonance structure in the πN data for this partial wave. The data [26] also show a total inelasticity at the 2 mb level, whereas the $2\pi N$ channel was found to be negligible [25]. It has been suggested [25] that this channel could have an important inelastic $3\pi N$ contribution. Since the measured $2\pi N$ cross-section is zero we have used the inelastic πN data with enlarged error bars instead of the $2\pi N$ data to pin down the $2\pi N$ D_{35} contributions. Even in this case we have found difficulties in the description of the D_{35} partial wave. The πN channel turns out to be strongly influenced by the u-channel nucleon and resonance contributions which give significant contributions to the real part of D_{35}. As can be seen in fig. 2 the C- and P-coupling calculations cannot give even a rough description of the experimental data [26]. The situation can be improved by either using a reduced nucleon cutoff Λ_N or by neglecting the nucleon u-channel contribution in the interaction kernel. The latter approximation has been used in the coupled-channel approach of Lutz *et al.* [33]. To illustrate this point we have carried out an additional fit for the C-coupling with the reduced cutoff $\Lambda_N = 0.91$ taking only the πN and $2\pi N$ data into account. The calculated χ^2 are $\chi^2_{\pi\pi} = 3.63$ and $\chi^2_{\pi 2\pi} = 7.87$, where the D_{35} data are also taken into account (note that all values in table 1 are calculated by neglecting these data points). The results for the D_{35} partial wave are shown in fig. 2 by the dotted line. In all calculations for D_{35} presented in fig. 2 the $D_{35}(1930)$ mass was found to be about 2050 MeV. One sees that the calculations with a reduced nucleon cutoff lead to a better description of the D_{35} data giving, however, a worse description of other πN partial-wave data. Note, that a reduction of the nucleon cutoff is required for a successful description of the lower-spin photoproduction multipoles [5,6], which also leads to a worsening in χ^2 for the πN elastic channel.

Finally, we conclude that the main features of the considered spin-$\frac{5}{2}$ partial waves except for D_{35} are well reproduced. From figs. 1-3 one can see that there is no significant difference between the conventional (8) and the Pascalutsa (11) spin-$\frac{5}{2}$ couplings.

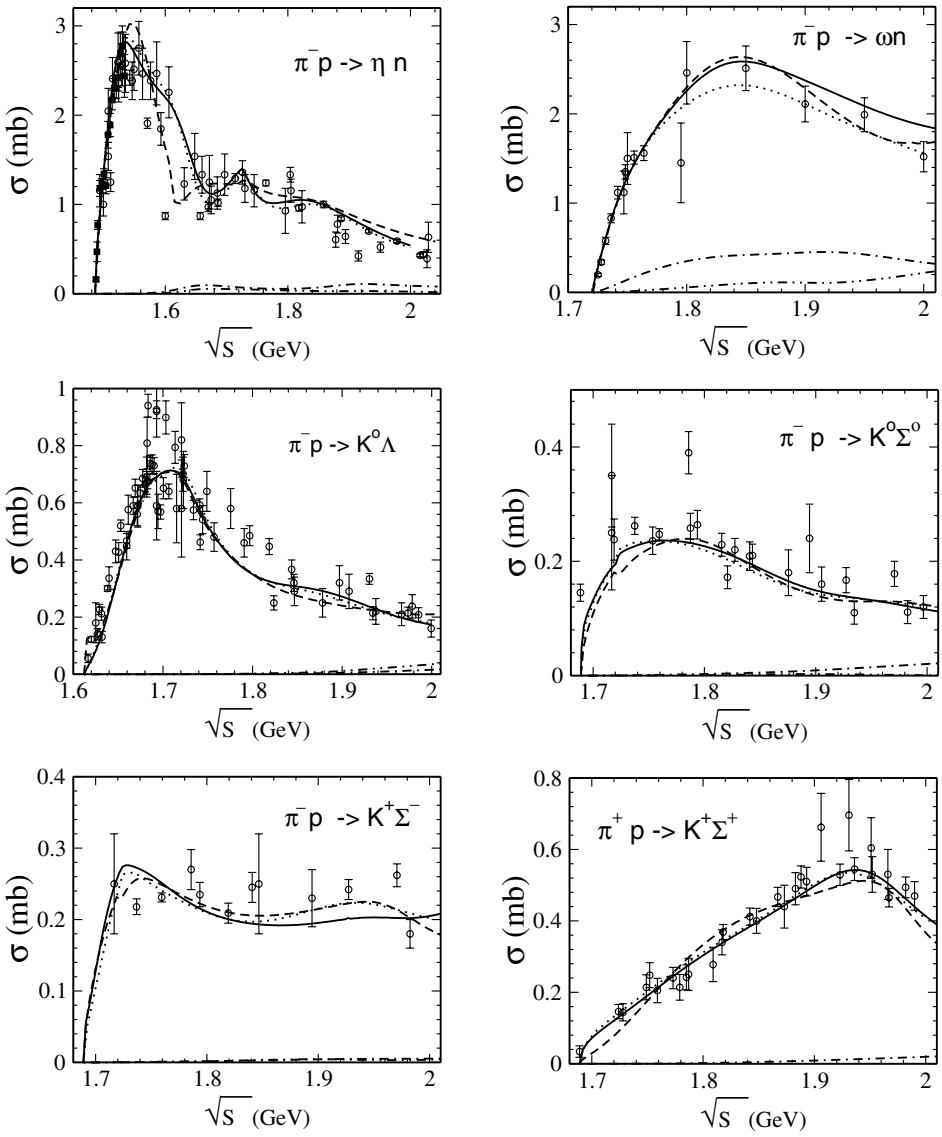

Fig. 4. The total cross-sections for the inelastic reactions. The solid (dashed) line corresponds to the C (P) result. The dotted line shows our previous results C-p-π+ [5]. The contributions from the spin-$\frac{5}{2}$ states are shown by dash-dotted (C) and dash-double-dotted (P) lines. For the data references see [5].

The parameters of the spin-$\frac{5}{2}$ resonances are presented in table 2. We note that the total resonance widths calculated here do not necessarily coincide with the full widths at half-maximum because of the energy dependence of the decay widths (4), (7) and the form factors used [5]. We do not show here the parameters of the $D_{35}(1930)$-resonance because of the problems in the $D_{35}(1930)$ partial wave. Although a good description of the experimental data is achieved some differences in the extracted resonance parameters for the C- and the P-coupling calculations exist.

We obtain a little lower mass for the $D_{15}(1675)$ as compared to that obtained by Manley and Saleski [28] and Vrana *et al.* [29], but in agreement with other findings [34,35]. The total width is found to be consistent with the results from [34,31,29]. In the ηN channel our calculations show a small ($\approx 0.6\%$) decay fraction which is somewhat higher than the value obtained by Batinić *et al.*: $0.1\pm 0.1\%$ [35], whereas Vrana *et al.* give another bound: $\pm 1\%$. We conclude that both fits give approximately the same results for the resonance masses and branching ratios.

The properties of the $F_{15}(1680)$ state are found to be in good agreement with the values recommended by [7]. We find a somewhat smaller branching ratio in the ηN channel as compared to that of [35]. However, the obtained value $R_{\eta N} = 0.1\%$ is again in agreement with the findings of Vrana *et al.* [29]: $\pm 1\%$. The parameters of the second $F_{15}(2000)$-resonance differ strongly in various analyses: Manley and Saleski [28] give 490 ± 310 MeV for the total decay width, while other studies [36,31] find it at the level of 95–170 MeV. Moreover, this state has not been identified in the investigations of [29,35]. Although we find different results for $\Gamma_{\rm tot}$ in the two independent

Table 2. Properties of the spin-$\frac{5}{2}$ resonances considered in the present calculation. Masses and total widths $\Gamma_{\rm tot}$ are given in MeV, the decay ratios R in percent of the total width. In brackets, the sign of the coupling is given (all πN couplings are chosen to be positive).

$L_{2I,2S}$	Mass	$\Gamma_{\rm tot}$	$R_{\pi N}$	$R_{2\pi N}$	$R_{\eta N}$	$R_{K\Lambda}$	$R_{K\Sigma}$	$R_{\omega N}$
$D_{15}(1675)$	1665	144	40.2	59.1(−)	0.6(−)	0.0(+)	$-0.04^{(a)}$	–
	1662	138	41.2	58.4(+)	0.4(−)	0.0(−)	$0.02^{(a)}$	–
$F_{15}(1680)$	1674	120	68.5	31.5(−)	0.1(+)	0.0(+)	$0.07^{(a)}$	–
	1669	122	65.8	34.2(+)	0.0(−)	0.0(+)	$0.13^{(a)}$	–
$F_{15}(2000)$	1981	361	9.0	84.0(+)	4.3(−)	$0.5^{(b)}$(−)	0.4(−)	2.2
	1986	488	9.5	88.2(−)	0.3(−)	0.1(+)	0.2(−)	1.7
$F_{35}(1905)$	1859	400	11.3	88.7(+)	–	–	$0.7^{(b)}$(+)	–
	1830	457	10.3	89.7(−)	–	–	0.0(+)	–

(a) The coupling is presented since the resonance is below threshold.

(b) Decay ratio in 0.1‰. The first line corresponds to C-calculation and the second one to P.

calculations, the branching ratios are close to each other. A small decay width of about 4.3% is found for the ηN channel (C). However, since the $F_{15}(2000)$-resonance is found to be strongly inelastic with 84–88% of inelasticity absorbed by the $2\pi N$ channel, more $2\pi N$ data above 1.8 GeV (cf. fig. 3) are needed for a reliable determination of the properties of this state.

The parameters of the $F_{35}(1905)$ state are in good agreement with [7]. Both fits give approximately the same result for the decay branching ratios.

All considered resonances have a rather small decay ratio to the ηN, $K\Lambda$, $K\Sigma$, and ωN channels. The only exception is the $F_{15}(2000)$-resonance where a small decay width to ηN has been found for the conventional coupling calculations.

In fig. 4 the results for ηN, $K\Lambda$, $K\Sigma$, and ωN total cross-sections are shown in comparison with best hadronic fit C-p-π+ from [5]. The main difference from the previous result is found in the ωN final state where a visible effect from the inclusion of the spin-$\frac{5}{2}$ resonances is found in the C-calculations. Although the $D_{15}(1675)$ and $F_{15}(1680)$ states are below the ω production threshold, they give noticeable contributions in the C-coupling calculations. This effect is, however, less pronounced in the P-calculations where the role of $D_{15}(1675)$ and $F_{15}(1680)$ are found to be less important.

Since the hadronic ωN data include about 115 data points the couplings to the ωN channel are not well constrained and inclusion of photoproduction data may change the situation [5]. Looking to the ω photoproduction reaction the new SAPHIR data may give an opportunity to distinguish between various reaction mechanisms. We are presently working on this [37].

4 Summary and outlook

We have performed a first investigation of the pion-induced reactions on the nucleon within the effective Lagrangian coupled-channels approach including spin-$\frac{5}{2}$ resonances. To investigate the influence of additional background from the spin-$\frac{3}{2}$ and -$\frac{5}{2}$ resonances, calculations using both the conventional and the Pascalutsa higher-spin couplings have been carried out. A good description of the available experimental data has been achieved in all πN, $2\pi N$, ηN, $K\Lambda$, $K\Sigma$, and ωN final states within both frameworks. The χ^2 is somewhat worse for the Pascalutsa prescription, but this is at least partly due to the absence of additional off-shell parameters in these couplings. In view of this ambiguity in the coupling it is gratifying to see that both coupling schemes lead to similar physical results for the baryon properties. The effective Lagrangian model used in our calculations imposes stringent physical constraints on the various channels and, in particular, on the interplay of the resonance and background contributions. The latter are generated by the same Lagrangian without any new unphysical parameters. Thus any remaining discrepancy between the data and the calculation points to the necessity to improve our understanding of the meson-baryon interactions further, for example, by including additional t-channel exchanges.

Apart from $2\pi N$ we find no significant contributions from other channels to the total πN inelasticities in the spin-$\frac{5}{2}$ waves. Nevertheless, the contributions from higher-spin resonances can be important in the ω production channel. More data on this reaction are highly desirable to establish the role of different reaction mechanisms.

We have found evidence for the $F_{15}(2000)$-resonance which is rated two-star by [7] and has not been included in the most recent resonance analysis by Vrana *et al.* [29]. However, more precise πN and $2\pi N$ data are necessary to identify this state more reliably in purely hadronic calculations.

For a complete description of the πN scattering up to higher energies the $J = \frac{5}{2}$ resonances are obviously needed. Compared to our previous study we arrive at a better description in the πN, ηN, and $\pi\Sigma$ channels for the conventional coupling calculations. Looking only at the lower partial waves, the improvement in πN is only possible due to the additional off-shell background from the spin-$\frac{5}{2}$ resonances. On the other hand, the missing background in the Pascalutsa prescription is compensated

by contributions from the D_{15} and F_{15} resonances allowing for a better description in the ηN and ωN final states.

We are proceeding with the extension of our model by performing a combined analysis of pion- and photon-induced reactions taking into account spin-$\frac{5}{2}$ states. Moreover, the decomposition of the $2\pi N$ channel into ρN, $\pi\Delta$ etc. states will be the subject of further investigations.

References

1. S. Capstick, W. Roberts, Prog. Part. Nucl. Phys. **45**, S241 (2000), nucl-th/0008028.
2. T. Feuster, U. Mosel, Phys. Rev. C **58**, 457 (1998).
3. T. Feuster, U. Mosel, Phys. Rev. C **59**, 460 (1999).
4. G. Penner, U. Mosel, Phys. Rev. C **65**, 055202 (2002).
5. G. Penner, U. Mosel, Phys. Rev. C **66**, 055211 (2002).
6. G. Penner, U. Mosel, Phys. Rev. C **66**, 055212 (2002).
7. K. Hagiwara *et al.*, Phys. Rev. D **66**, 010001 (2002), `http://pdg.lbl.gov`.
8. R.A. Arndt, W.J. Briscoe, I.I. Strakovsky, R.L. Workman, Phys. Rev. C **66**, 055213 (2002).
9. D. Drechsel, O. Hanstein, S.S. Kamalov, L. Tiator, Nucl. Phys. A **645**, 145 (1999); S.S. Kamalov, D. Drechsel, O. Hanstein, L. Tiator, S.N. Yang, Nucl. Phys. A **684**, 321c (2001).
10. A.I. Titov, T.-S.H. Lee, Phys. Rev. C **66**, 015204 (2002); B. Kämpfer, A.I. Titov, B.L. Reznik, *PANIC02, Osaka, Japan (2002)*, Nucl. Phys. A **721**, 583 (2003), nucl-th/0211078.
11. W. Rarita, J. Schwinger, Phys. Rev. **60**, 61 (1941).
12. G. Penner, PhD Thesis, Universität Gießen, 2002, available via `http://theorie.physik.uni-giessen.de`.
13. B.C. Pearce, B.K. Jennings, Nucl. Phys. A **528**, 655 (1991).
14. C. Sauermann, B.L. Friman, W. Nörenberg, Phys. Lett. B **341**, 261 (1995); C. Deutsch-Sauermann, B. Friman, W. Nörenberg, Phys. Lett. B **409**, 51 (1997).
15. M. Zétényi, Gy. Wolf, nucl-th/0103062.
16. J.C. David, C. Fayard, G.H. Lamot, B. Saghai, Phys. Rev. C **53**, 2613 (1996).
17. B.S. Han, M.K. Cheoun, K.S. Kim, I.-T. Cheon, Nucl. Phys. A **691**, 713 (2001).
18. L.M. Nath, B. Etemadi, J.D. Kimel, Phys. Rev. D **3**, 2153 (1971); L.M. Nath, B.K. Bhattacharyya, Z. Phys. C **5**, 9 (1980).
19. M. Benmerrouche, R.M. Davidson, N.C. Mukhopadhyay, Phys. Rev. C **39**, 2339 (1989); R.M. Davidson, N.C. Mukhopadhyay, R. Wittman, Phys. Rev. Lett. **56**, 804 (1986).
20. B.J. Read, Nucl. Phys. B **52**, 565 (1973).
21. V. Pascalutsa, Phys. Rev. D **58**, 096002 (1998); V. Pascalutsa, R. Timmermans, Phys. Rev. C **60**, 042201 (1999).
22. V. Pascalutsa, Phys. Lett. B **503**, 85 (2001).
23. V. Pascalutsa, J.A. Tjon, Phys. Rev. C **61**, 054003 (2000).
24. A.D. Lahiff, I.R. Afnan, Phys. Rev. C **60**, 024608 (1999).
25. D.M. Manley, R.A. Arndt, Y. Goradia, V.L. Teplitz, Phys. Rev. D **30**, 904 (1984).
26. M.M. Pavan, R.A. Arndt, I.I. Strakovsky, R.L. Workman, Phys. Scr. **T87**, 62 (2000); nucl-th/9807087; R.A. Arndt, I.I. Strakovsky, R.L. Workman, M.M. Pavan, Phys. Rev. C **52**, 2120 (1995), updates available via `http://gwdac.phys.gwu.edu/`.
27. Available via `http://www.uni-giessen.de/~gd1267/`.
28. D.M. Manley, E.M. Saleski, Phys. Rev. D **45**, 4002 (1992).
29. T.P. Vrana, S.A. Dytman, T.-S.H. Lee, Phys. Rep. **328**, 181 (2000).
30. R.E. Cutkosky, S. Wang, Phys. Rev. D **42**, 235 (1990).
31. G. Höhler, F. Kaiser, R. Koch, E. Pietarinen, *Handbook of Pion-Nucleon Scattering*, Landolt-Börnstein, Phys. Data **12-1** (1979).
32. R.L. Kelly, R.E. Cutkosky, Phys. Rev. D **20**, 2782 (1979).
33. M.F.M Lutz, Gy. Wolf, B. Friman, Nucl. Phys. A **706**, 431 (2002).
34. R.E. Cutkosky, C.P. Forsyth, J.B. Babcock, R.L. Kelly, R.E. Hendrick, in *Baryon 1980, Proceedings of the 4th International Conference on Baryon Resonances, Toronto, Canada, July 14-16, 1980*, edited by N. Isgur (University of Toronto Press, Toronto, 1981) p. 19; R.E. Cutkosky, C.P. Forsyth, R.E. Hendrick, R.L. Kelly, Phys. Rev. D **20**, 2839 (1979).
35. M. Batinić, I. Šlaus, A. Švarc, B.M.K. Nefkens, Phys. Rev. C **51**, 2310 (1995); **57**, 1004 (1998)(E); nucl-th/9703023; M. Clajus, B.M.K. Nefkens, πN Newslett. **7**, 76 (1992).
36. R.A. Arndt, I.I. Strakovsky, R.L. Workman, M.M. Pavan, Phys. Rev. C **52**, 2120 (1995).
37. V. Shklyar, G. Mosel, U. Mosel, in preparation.